PHYSICAL AND CHEMICAL PROPERTIES AND PHOTOCATALYTIC ACTIVITY OF NANOSTRUCTURED TiO2/CdS FILMS

M. A. Zhukovskiy,[a] N. P. Smirnova,[a*] I. A. Rusetsky,[b] G. Ya. Kolbasov,[b] and A. M. Eremenko[a]

UDC 544.526+54.057;620.3

Mesoporous titanium dioxide films obtained by the sol/gel template method are used as supports for making TiO2/CdS nanoheterostructures. We show that the photocatalytic method results in formation of smaller CdS nanoparticles than chemical deposition. Photoelectrochemical measurements show more efficient spatial separation of photogenerated charges between components of the photocatalytically produced TiO2/CdS films, and consequently their participation in redox transformation of the xanthene dye Rose Bengal when exposed to UV light leads to higher quantum yields.

***Keywords:** mesoporous film, photochemical deposition, TiO2/CdS nanostructure, photocatalysis, Rose Bengal.*

Introduction. Intensive basic and applied research on nanostructured titanium dioxide films, deposited on the surface of glass, metals, organic polymers, and other materials, has been stimulated by the wide-ranging prospects for their application in modern technologies for solar energy conversion [1–3]. The solution to the problem of improving the efficiency of photosensitive systems based on porous nanostructured TiO2 films is mainly associated with expansion of the range of their photosensitivity into the visible spectral region and reducing undesirable losses of photogenerated charges in recombination processes. One promising route for comprehensive solution of this problem is to design binary systems consisting of titanium dioxide and another photosensitive component, such as for example a narrow-band semiconductor with the conduction band at higher energy than in TiO2, or metal nanoparticles. The most impressive results have been achieved when using metal sulfide (MS) semiconductors (CdS, PbS, Bi2S3) as sensitizers of titanium dioxide in photoanodes of photoelectrochemical cells [4, 5]. Along with conventional "chemical" synthesis methods for MS/TiO2 nanocomposites, photochemical approaches can be used that are based on the capability of TiO2 nanoparticles for photocatalytic conversions of sulfur-containing compounds [6–8].

The high rate of spatial separation of unlike photogenerated charges between components of CdS/TiO2 nanostructures results in their elevated activity in reactions of evolution of hydrogen from aqueous solutions of electron donors, degradation of organic dyes, tetrachlorobenzene, reduction of methyl viologen, and oxidation of indole [9–12]. It was established earlier by pulsed laser photolysis [13] that spatial separation of photogenerated charges between components of photocatalytically produced TiO2/CdS nanostructures occurs an order of magnitude more efficiently than in nanostructures of analogous composition obtained chemically (3–5 μs) and their recombination occurs significantly more slowly (>100 μs) [13].

This paper focuses on study of the effect of the synthesis method for TiO2/CdS nanoheterojunctions on their structure, photoelectrochemical characteristics, and photocatalytic activity in the reaction of oxidation of the xanthene dye Rose Bengal (RB):
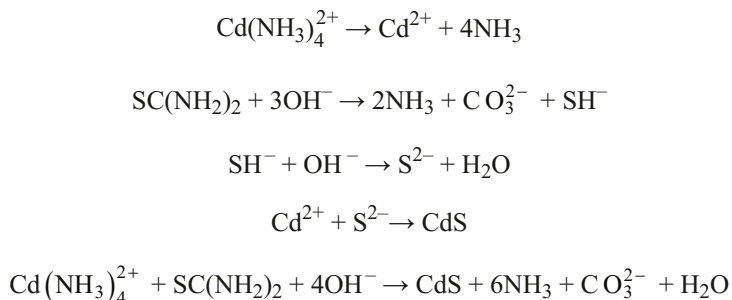

$X1 - X4 = I$
$X5 - X8 = Cl$

_____
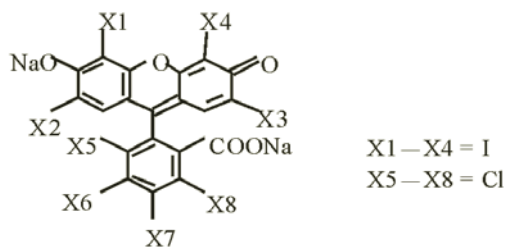
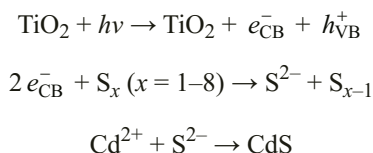[*]To whom correspondence should be addressed.

[a]A. A. Chuiko Institute of Surface Chemistry, National Academy of Sciences of Ukraine, 17 General Naumov Str., Kiev, 03164, Ukraine; e-mail: smirnat@i.ua; [b]V. I. Vernadsky Institute of General and Inorganic Chemistry, National Academy of Sciences of Ukraine, Kiev. Translated from Zhurnal Prikladnoi Spektroskopii, Vol. 81, No. 2, pp. 244–249, March–April, 2014. Original article submitted June 19, 2013.

Experimental Section. Mesoporous titanium dioxide films were prepared by the sol/gel method: hydrolysis of titanium isopropoxide $Ti(OPr)_4^{iso}$ in the presence of Pluronic P123 (triblock copolymer of ethylene and propylene oxides) as the template and acetylacetone as the chelating agent to slow down the rate of hydrolysis of the titanium alkoxide [14]. We used the dip-coating method to deposit the films on glass substrates for the photocatalytic studies and on titanium foil for the photoelectrochemical studies. We used six-layer coatings obtained by successive deposition of the films six times, after drying each layer in air. After deposition, the films were hydrolyzed in air and calcined in a muffle furnace at 400°C.

The TiO$_2$/CdS structures were obtained by chemical (chem) and photochemical (photo) deposition. In order to obtain composite TiO$_2$/CdS(chem) films, the original titanium dioxide films were dipped in an aqueous solution containing cadmium acetate and thiourea, after which the pH of the solution was raised with ammonia to pH 12–13. The process of cadmium sulfide deposition is based on slow release of Cd^{2+} ions from the $Cd(NH_3)_4^{2+}$ complex, which are adsorbed on the titanium dioxide film, and S^{2-} ions formed in decomposition of thiourea [15]. This process can be represented schematically as:

$$Cd(NH_3)_4^{2+} \rightarrow Cd^{2+} + 4NH_3$$

$$SC(NH_2)_2 + 3OH^- \rightarrow 2NH_3 + CO_3^{2-} + SH^-$$

$$SH^- + OH^- \rightarrow S^{2-} + H_2O$$

$$Cd^{2+} + S^{2-} \rightarrow CdS$$

$$Cd(NH_3)_4^{2+} + SC(NH_2)_2 + 4OH^- \rightarrow CdS + 6NH_3 + CO_3^{2-} + H_2O$$

Photochemical deposition of CdS was carried out with exposure to UV light (λ = 310–370 nm) of TiO$_2$ films dipped in a solution of sulfur (S$_8$) and Cd(CH$_3$COO)$_2$ in anhydrous ethanol in an evacuated glass reactor:

$$TiO_2 + h\nu \rightarrow TiO_2 + e_{CB}^- + h_{VB}^+$$

$$2\,e_{CB}^- + S_x\,(x = 1\text{–}8) \rightarrow S^{2-} + S_{x-1}$$

$$Cd^{2+} + S^{2-} \rightarrow CdS$$

Electron micrographs of the surface of the mesoporous films were obtained using a LEO-1530 scanning electron microscope (SEM) with accelerating voltage 100 kV.

To study the photocatalytic activity of the samples, we used the test reaction of Rose Bengal degradation. Photooxidation of Rose Bengal with concentration $C_m = 1 \cdot 10^{-5}$ mol/L in aqueous solutions was carried out in a water-cooled 20 mL quartz reactor with vigorous stirring and free access of air. The aqueous solutions of the dye were irradiated in the presence of the photocatalysts by near-UV light (λ = 310–390 nm) from a DRSh-1000 high pressure mercury lamp at pH 6–7. The Rose Bengal concentration was monitored from the change in the intensity of the absorption spectrum at λ = 529 nm during irradiation using a Lambda 35 UV-Vis spectrophotometer (Perkin Elmer).

Results and Discussion. As we see from micrographs of the surface of TiO$_2$/CdS films, in photocatalytic deposition of cadmium sulfide, islands are formed on the surface of nanocrystalline titanium dioxide films which consist of CdS aggregates of length 100–200 nm (Fig. 1a). With chemical deposition, CdS is uniformly distributed over the entire surface of the film as bulk particles of size up to 1 μm (Fig. 1b). These data are consistent with the results obtained previously by atomic force microscopy [14], which suggest that during photocatalytic reduction of sulfur on the surface of TiO$_2$ films in the presence of cadmium(II) acetate, elongated nanoaggregates of cadmium sulfide are formed that consist of CdS nanoparticles that are smaller (5–6 nm) than for conventional chemical deposition (>20 nm) of cadmium sulfide.

In the Raman spectra of TiO$_2$/CdS(chem) samples, we see characteristic bands at ~300 and ~600 cm^{-1} (Fig. 2), which correspond to a longitudinal optical phonon (LO) and its second order mode (2LO) in CdS [16]. In the spectrum of the sample synthesized photocatalytically, an additional weak peak can be assigned to a transverse optical phonon (TO) or a surface optical phonon (SO). Its presence may indicate somewhat smaller CdS particles in the TiO$_2$/CdS (photo) sample compared with the product of conventional chemical synthesis, and also more significant structural disordering (high degree of amorphization) of the cadmium sulfide formed during photocatalytic reduction of sulfur by ethanol on the surface of mesoporous TiO$_2$. The TiO$_2$ films deposited on a titanium plate, as is consistent with the bandgap width $\Delta E_g > 3.2$ eV characteristic for titanium dioxide (anatase), exhibits photosensitivity in the region $\lambda < 400$ nm.
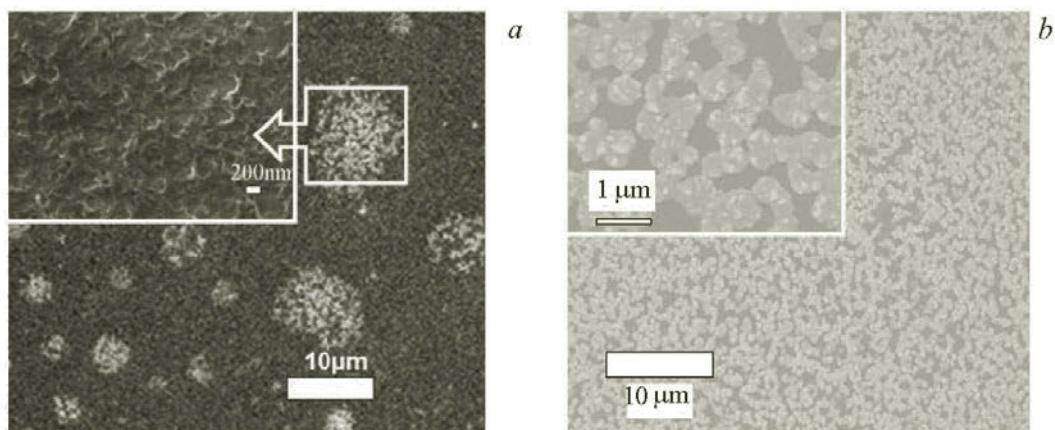
Fig. 1. SEM image of the surface of TiO$_2$/CdS films synthesized by photochemical (a) and chemical (b) deposition of cadmium sulfide.
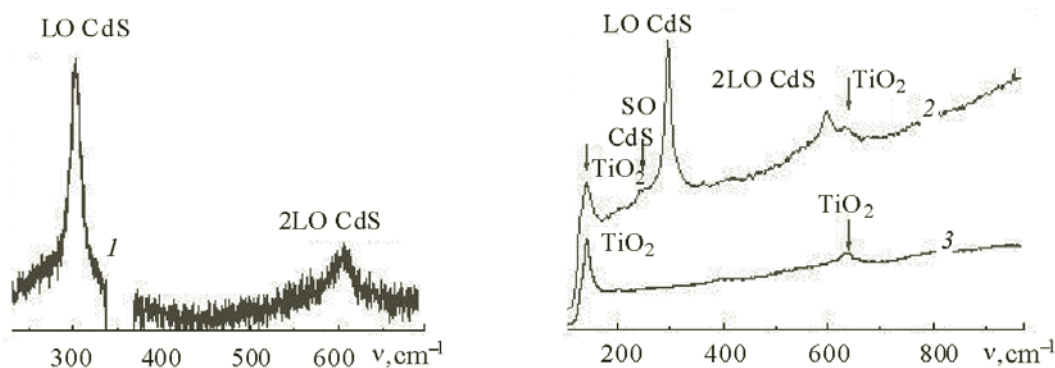

Fig. 2. Raman spectra of TiO$_2$/CdS samples synthesized by chemical (1) and photocatalytic (2) deposition of cadmium sulfide on the surface of mesoporous titanium dioxide; 3) Raman spectrum of the original TiO$_2$.

Deposition on the TiO$_2$ surface of cadmium sulfide particles ($\Delta E_g > 2.4$ eV) leads to an increase in the photocurrent quantum yield in the UV region and appearance of photosensitivity to light in the visible region of the spectrum ($\lambda > 400$ nm). In this case, the composite TiO$_2$/CdS(photo) is characterized by a higher quantum yield than for TiO$_2$/CdS(chem) (Fig. 3a). The increase in the photocurrent quantum yield in the UV region may suggest more efficient separation of photogenerated charges due to CdS particles accumulating holes from the TiO$_2$ nanoparticles (suppression of recombination processes). The reason for the high efficiency of TiO$_2$/CdS(photo) electrodes is their formation by photodeposition of cadmium sulfide directly on the active sites of titanium dioxide, which provides electronic contact between the components of the heterostructure and prevents recombination processes. In contrast to nanocomposites obtained photochemically, in TiO$_2$/CdS(chem) electrodes the cadmium sulfide is randomly deposited on the TiO$_2$ surface, where both separation of unlike charges and recombination processes occur between particles of such a structure.

For these systems, we observe an extremal dependence of the photocurrent quantum yield with a shift of the maximum toward higher energies (Fig. 3a). The shift of the maximum is the result of the balance between absorption and recombination processes and is due to the decrease in recombination losses of charge carriers, also including a decrease in the cathode photocurrent, and consequently the photosensitivity of the heterostructure increases in the UV region [17]. The drop in photocurrent in the long-wavelength region of the spectrum is due to the decrease in the absorption coefficient near the intrinsic absorption band edge of TiO$_2$ and CdS. The drop in photocurrent in the short-wavelength region of the spectrum may be the result of recombination losses of photogenerated charge carriers and the effect of photocathode processes [17].
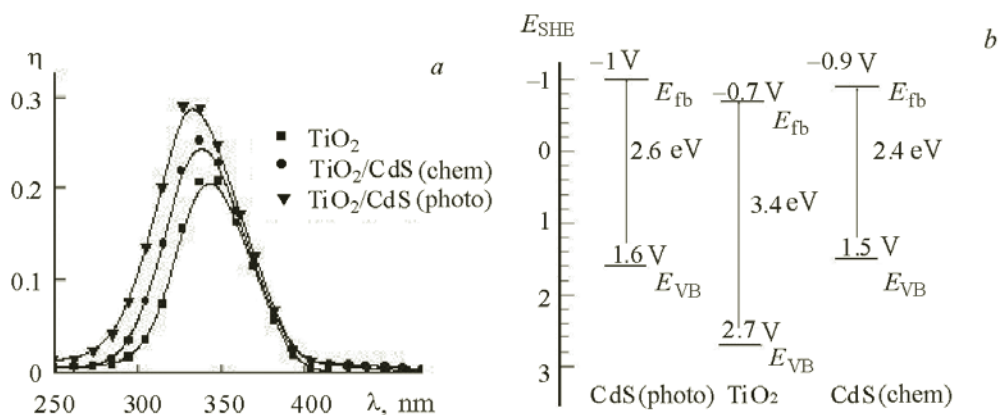
Fig. 3. Photocurrent quantum yield (a) and energy diagram for TiO_2, $TiO_2/CdS(chem)$, and $TiO_2/CdS(photo)$ electrodes (b).

TABLE 1. Quantum Yield (Φ) for Photooxidation of Rose Bengal Dye in the Presence of TiO_2 and TiO_2/CdS Films

Photocatalyst	λ_{irr}, nm	$\Phi \cdot 10^{-5}$	λ_{irr}, nm	$\Phi \cdot 10^{-5}$
No photocatalyst		1.11		1.19
TiO_2	310–390	1.59	> 460	1.74
$TiO_2/CdS(chem)$		1.86		1.85
$TiO_2/CdS(photo)$		2.44		1.80

To estimate the energy parameters of the studied systems from the dependences of the photocurrent quantum yield h on the potential of the TiO_2, $TiO_2/CdS(chem)$, and $TiO_2/CdS(photo)$ electrodes, we determined the flat-band potentials (E_{fb}) given in Table 1. We plotted the energy diagrams (the position of the levels is represented relative to the standard hydrogen electrode (SHE)), which let us estimate the efficiency of these systems in photochemical processes (Fig. 3b). For $TiO_2/CdS(photo)$ films, we note an anode shift of the valence band energy by 0.1 V, which suggests enhanced oxidizability of photogenerated holes in the valence band and increased catalytic activity of these materials compared with $TiO_2/CdS(chem)$ during photooxidation processes.

Photocatalytic oxidation of Rose Bengal dye in the presence of TiO_2/CdS films. Reactions of photocatalytic oxidation/reduction of the dyes are used as typical test reactions for comparison of the photocatalytic properties of different types of semiconductor materials. The synthesized TiO_2/CdS nanostructures were tested using the reaction of oxidation of the halogenated fluorescein Rose Bengal. The oxidation potential of the excited state of Rose Bengal calculated in [18] is –1.33 V (relative to the SHE), which makes electron transfer from the dye to the conduction band of TiO_2 and TiO_2/CdS nanostructures thermodynamically favorable (Fig. 3b). The course of the photochemical processes was observed from the decrease in the intensity of absorption by the dye (Fig. 4a and c); the kinetic curves for photodecomposition are shown in Fig. 4b, d and the quantum yields of the reaction are given in Table 1.

On exposure to UV light, the greatest photocatalytic activity in the reaction of Rose Bengal degradation is demonstrated by $TiO_2/CdS(photo)$ nanoheterostructures. Conversion of the dye after 60 minutes of exposure is 25–30% higher than for the analogous nanoheterostructure formed chemically, and 70–80% higher than for the original nanocrystalline titanium dioxide film (Fig. 4b).

When aqueous solutions of Rose Bengal are exposed to visible light, we observe their gradual decolorization due to photochemical degradation of the dye. In the presence of nanocrystalline titanium dioxide films, this process occurs several times faster (Fig. 4c and d). Acceleration of photodegradation of the dye in this case is probably due to electron transfer from its singlet-excited molecules to TiO_2 nanoparticles [18]. Thus Rose Bengal can act as a sensitizer for oxidation/reduction processes with participation of titanium dioxide films for visible light.
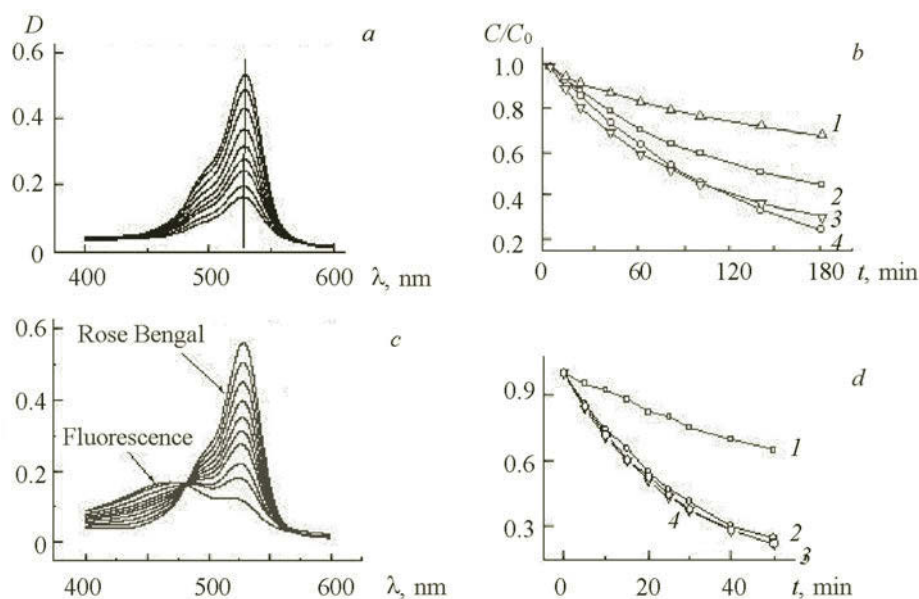
Fig. 4. Transformation of absorption spectrum of Rose Bengal dye in an air-saturated alkaline aqueous solution when exposed to UV with l = 310–390 nm (a) and visible light with l > 460 nm (c) in the presence of a TiO$_2$/CdS(photo) film; the kinetic curves for photodegradation of Rose Bengal when exposed to UV (b) and visible light (d) with no semiconductor (1) and in the presence of TiO$_2$ (2), TiO$_2$/CdS(photo) (3), and TiO$_2$/CdS(chem) (4) films.

Deposition of CdS nanoparticles on the surface of mesoporous TiO$_2$ films has practically no effect on the rate and extent of Rose Bengal degradation, possibly due to competitive absorption of light in the same spectral range by both the semiconductor and the dye. It was previously noted [19] that photodecomposition of rhodamine B adsorbed on CdS occurs mainly as a result of absorption of light by the dye itself, and to a lesser extent by excitation to the absorption band of CdS, and practically does not involve the dye in solution. Evidence that the process occurs through a photoinduced electron transfer step when exposed to visible light in the presence of both TiO$_2$ and TiO$_2$/CdS nanocomposites comes from the gradual formation of an absorption band in the spectrum that is characteristic for the completely dehalogenated form of the dye, fluorescein (Fig. 5c). We know that dehalogenation of fluorescein derivatives occurs through an intermediate step of formation of the triplet-excited form of the dye, followed by cleavage of the halogen groups [19], similar to the process of de-ethylation of rhodamine dyes when exposed to visible light in the presence of cadmium sulfide [20] or TiO$_2$ [21].

Conclusions. We have established that the higher efficiency of TiO$_2$/CdS electrodes fabricated by photochemical deposition, compared with chemical deposition, for obtaining a photocurrent is due to chemical contact between the components of the heterostructure, which significantly decreases the losses of charge carriers in recombination processes. Redox conversions of the dye Rose Bengal when exposed to UV light in the presence of TiO$_2$/CdS(photo) film nanoheterostructures occur with higher quantum yields than for TiO$_2$/CdS(chem), due to the more efficient separation of photogenerated charges.

REFERENCES

1. K. Rajeshwar and N. R. de Tacconi, *Chem. Soc. Rev.*, **38**, 1984–1998 (2009).
2. A. Fujishima, X. Zhang, and D. A. Tryk, *Surf. Sci. Rep.*, **63**, 515–568 (2008).
3. R. Vogel, P. Meredith, I. Kartini, J. Rishes, A. Bishop, N. Heckenberg, M. Trau, and H. Rubensztein-Dulop, *Chem. Phys. Chem.*, **4**, 595–603 (2003).
4. H. Tada, T. Mitsui, T. Kiyonaga, T. Akita, and K. Tanaka, *Nature Mater.*, **5**, 782–786 (2006).
5. J. L. Blackburn, D. C. Selmarten, and A. J. Nozik, *J. Phys. Chem. B*, **107**, 14154–14157 (2003).
6. V. V. Shvalagin, A. L. Stroyuk, and S. Ya. Kuchmii, *Teor. Éksp. Khim.*, **43**, 215–219 (2007).

7. H. Tada, M. Fujishima, and H. Kobayashi, *Chem. Soc. Rev.*, **40**, 4232–4243 (2011).

8. M. A. Zhukovskiy, A. L. Stroyuk, V. V. Shvalagin, N. P. Smirnova, O. S. Lytvyn, and A. M. Eremenko, *J. Photochem. Photobiol. A: Chem.*, **203**, 137–144 (2009).

9. J. C. Kim, J. Choi, Y. B. Lee, J. H. Hong, J. I. Lee, J. W. Yang, W. I. Lee, and N. H. Hur, *Chem. Commun.*, No. 48, 5024–5026 (2006).

10. Y. Bessekhouad, D. Robert, J. V. Weber, and N. Chaoui, *J. Photochem. Photobiol. A*, **163**, 569–580 (2004).

11. H. Yin, Y. Wada, T. Kitamura, T. Sakata, H. Mori, and S. Yanagida, *Chem. Lett.*, No. 4, 334–335 (2001).

12. W.-W. So, K.-J. Kim, and S.-J. Moon, *Int. J. Hydrogen Energy*, **29**, 229–234 (2004).

13. A. L. Stroyuk, S. Ya. Kuchmii, M. A. Zhukovskii, N. P. Smirnova, E. M. Glebov, V. P. Grivin, and V. F. Plyusnin, *Teor. Éksp. Khim.*, **45**, 284–291 (2009).

14. Yu. Gnatyuyk, M. Zhukovskiy, N. Smirnova, A. Eremenko, A. Guobiené, and S. Tamulevicius, in: Yu. L. Zub and V. G. Kessler (Eds.), *Sol-Gel Methods for Materials Processing, NATO Science for Peace and Security Series. C: Environmental Security* (2008), pp. 315–321.

15. J. M. Dona and J. Herrero, *J. Electrochem. Soc.*, **139**, 2810–2814 (1992).

16. P. Rodriguez, N. Munoz-Aguirre, E. San-Marten Martinez, G. Gonzalez de la Cruz, S. A. Tomas, and O. Zelaya Angel, *J. Cryst. Growth*, **310**, 160–164 (2008).

17. G. Ya. Kolbasov and A. V. Gorodyskii, *Photostimulated Charge Transfer Processes in a Semiconductor/Electrolyte System* [in Russian], Naukova Dumka, Kiev (1993).

18. M. Asha Jhonsi, A. Kathiravan, and R. Renganathan, *J. Mol. Struct.*, **921**, 279–284 (2009).

19. M. A. Rauf, N. Marzouki, and K. B. Krbahti, *J. Hazard. Mater.*, **159**, 602–609 (2008).

20. T. Watanabe, T. Takizawa, and K. Honda, *J. Phys. Chem. B*, **81**, 1845–1851 (1977).

21. T. Wu, G. Liu, J. Zhao, H. Hidaka, and N. Serpone, *J. Phys. Chem. B*, **102**, 5845–5851 (1998).